# Electronic Supplementary Information

# Mechanochromic Luminescence Covalent Organic Frameworks for High Selective Hydroxyl Radicals Detection

Wei Liu [a], Yuping Cao [a], Wenzhuang Wang [b], Deyan Gong [a], Ting Cao [a], Jing Qian [a], Kanwal Iqbal [a,c], Wenwu Qin [a*], Huichen Guo [d*]

[a] Key Laboratory of Nonferrous Metal Chemistry and Resources Utilization of Gansu Province and State Key Laboratory of Applied Organic Chemistry, College of Chemistry and Chemical Engineering, Lanzhou University, Lanzhou 730000, P. R. China

[b] Cuiying Honors College, Lanzhou University, Lanzhou 730000, P. R. China.

[c] Department of chemistry Faculty of Basic Sciences, Sardar Bahadur Khan University 87300Quetta, Pakistan

[d] State Key Laboratory of Veterinary Etiological Biology and Key Laboratory of Animal Virology of Ministry of Agriculture, Lanzhou Veterinary Research Institute, Chinese Academy of Agricultural Sciences, Xujiaping 1, Lanzhou, Gansu Province 730046, P. R. China

**Table of contents**

**Figure S7.** UV/vis absorption spectra of COF-TpMA (MC), Tp and MA.

**Figure S8.** AA stacking and AB stacking structure of COF-TpMA (MC).

**Figure S9.** $N_2$ adsorption-desorption isotherms and pore size distribution profiles of COF-TpMA (MC).

**Figure S10.** TGA curve of COF-TpMA (MC).

**Figure S11.** Photo of products under sunlight and UV light of COF-TpMA (MC) at 12 grinding.

**Figure S12.** Fluorescence micrographs of COF-TpMA (MC) at 12 h grinding.

**Figure S13.** The PXRD spectra of COF-TpMA (MC) and grinding 12 h product.

**Figure S14.** Absorption spectra of COF-TpMA (MC) in different concentration of •OH.

**Figure S15.** Absorption changes of COFs-TpMA (MC) with •OH and the linear relationship between the •OH concentration range (0-10 μM) at 283 nm.

**Figure S16.** Fluorescence changes of COFs-TpMA (MC) with •OH and the linear relationship between the •OH concentration range (0-10 μM) at 530 nm (λex = 380 nm).

**Figure S17.** Time-dependent fluorescent response at 530 nm (λex = 380 nm) for COF-TpMA (10 μM) upon addition of 50 equiv of •OH.

**Figure S18.** Specific selectivity of COF-TpMA (MC) reacted with different reactive oxygen species.

**Figure S19.** Representative fluorescence decays of COF-TpMA (10 μM) in the absence and presence of different concentration of •OH.

**Figure S20.** Best fits of Eq $F/F_0=1+Kq$ to the emission fluorometric titration data of COF-TpMA

**Figure S21.** Effects of COF-TpMA at varied concentrations on the viability of BHK cells.

**5. Supporting Tables**

**Table S1.** Fractional atomic coordinates for the unit cell of COF-TpMA of AA stacking.

**Table S2.** Fractional atomic coordinates for the unit cell of COF-TpMA of AB stacking.

**Table S3.** Analyses of decay times $\tau_1$, $\tau_2$ and $\tau_3$, and the relative amplitude $\alpha_i$ (%) at different concentration of •OH.

**6. Supporting References**

## 1. Materials.

Unless otherwise noted, all reagents and solvents were obtained from commercial sources and used directly without further purification. Ethyl acetate (EA), Dichloromethane (DC), Petroleum ether (PE), Cyclohexane (CYH), Acetonitrile ($CH_3CN$), Trichloromethane ($CHCl_3$), Tetrahydrofuran (THF), Acetone, Ethanol (EtOH) and Methyl alcohol ($CH_3OH$) were analytical reagent grade. Phloroglucinol ($C_6H_6O_3$, 99%), Hexamethylenetetramine ($C_6H_{12}N_4$, ≥99.0%), Melamine (Me, 99%), dimethyl sulfoxide (DMSO), Trifluoroacetic acid ($C_2HF_3O_2$, 99%). 1, 3, 5-Triformylphloroglucinol (Tp) was synthesized according to a reported procedure.[1] Deuterated solvents for NMR measurement were obtained from Aldrich. Distilled water was used in the experiments. All titration and selectivity experiment of COF-TpMA (MC) was diluted in DMSO/PBS buffer (1:9, v/v, 20 mM, pH 7.4) with 3 mM CTAB and then kept at 37 °C in a thermostatic water bath. Other chemicals used in this study were analytical reagent grade.

**2. Methods and Instruments.**

$^{1}H$ spectra were recorded on a Bruker 400M Hz spectrometer, where chemical shifts (δ in ppm) were determined with a residual proton of the solvent as standard. FTIR spectra of the materials were conducted within the 4000–400 $cm^{-1}$ wavenumber range by using a Nicolet 6700. FTIR spectrometer with the KBr pellet technique. Elemental analyses were carried out on an Elemental model Vario EL analyzer. SEM images were obtained with a Zeiss DSM 950 scanning electron microscope. The TEM samples were prepared by drop-casting the sample from acetone on micro grids TEM Window (TED PELLA, INC. 200 mesh). Powder X-ray diffraction data were recorded on a PANalytical BV Empyrean diffractometer by depositing powder on glass substrate, from $2\theta$ = 3.0° to 40° with 0.02° increment at 25 °C, operating at 40 kV and 100 mA, using CuKa radiation source (1.5406 A). Thermogravimetric analysis (TGA) was performed on a TA Q500 thermogravimeter by measuring the weight loss while heating at a rate of 10 °C • $min^{-1}$ within a temperature range of 30-800 °C under nitrogen. Nitrogen sorption isotherms were measured at 77 K with a JW-BK 132F analyzer. Before measurement, the samples were degassed in vacuum at 100 °C for more than 10 h. The Brunauer-Emmett-Teller (BET) method was utilized to calculate the specific surface areas and pore volume, the NLDFT method was applied for the estimation of pore size distribution. UV-vis absorption spectra were obtained on a Varian UV-Cary5000 spectrophotometer. Fluorescence emission spectra were collected using Hitachi F-7000 spectrofluorimeter with 1 cm quartz cells. Instruments FSL920 fluorescence spectrometer with a 450 W Xe arc lamp as the

steady-state excitation source and an Nd-pumped OPOlette laser as the excitation source for lifetime measurements.

## 3. Experimental Details.

### A. Synthesis of COF-TpMA (MC).

The solvent-free MC syntheses of COF-TpMA were carried out using Schiff base aldehyde-amine condensation reactions. In a typical synthesis 1,3,5-trimethylresorcinol (Tp) (0.238 mmol, 50 mg) and melamine (0.247 mmol, 31.2 mg) were mixed and grinded with a pestle at room temperature, and with 1-2 drops of methanol grounded.[2] Every three hours we detected the reaction via FT-IR spectroscopy, fluorescence spectra, PXRD and fluorescence microscopy. The monomers were ground for three hours to obtain a light yellow powder and found that these powders were mixture of oligomer form and some unreacted starting materials with a yellow-green fluorescence. As time goes on, the color changed to yellow (6 h), which may be due to the increase in the number of units and conjugation, and eventually a brown-yellow color was observed in the final 12 hours, indicating that COF was formed completely. The brown-yellow powders collected after 12 hours were washed three to four times with hot water, methanol and dichloromethane to remove some unreacted raw materials and oligomerization impurities, and then dried at 80 °C under vacuum for 24 hours. The brown-yellow powders with orange fluorescence were obtained; the isolated yield was 60%. In order to ensure the stability of COF-TpMA (MC), the dry powdered samples were characterized by powder X-ray diffraction (PXRD), thermogravimetric analysis (TGA), Fourier transform IR (FT-IR) spectroscopy, Transmission electron microscopy (TEM) and Scanning electron microscope (SEM).

**B. General method for measurements of quantum yield.**

For the determination of the fluorescence quantum yields ϕf of COF-TpMA (MC), only dilute solutions with an absorbance below 0.1 at the excitation wavelength were used. Quinine sulfate / 0.5 M $H_2SO_4$ ($\Phi_f$ = 0.55) was used as fluorescence standard. [3]

**C. Fluorescence Spectroscopy.**

The COF-TpMA (MC) obtained by grinding 12 h was used for detecting hydroxyl radicals. The sample was excited at 380 nm, and the emission was collected from 400 to 700 nm. The experiments for •OH detection was all carried out three times. Probe COF-TpMA (MC) (3 mg) were dissolved in DMSO/PBS buffer (1:9, v/v, 20 mM, pH 7.4) with 3 mM CTAB to afford the stock solution (0.6 mg/mL). To detect •OH by COF-TpMA (MC) probe, 3 mL of standard solution (pH = 7.4) was first added into the cuvette, then •OH was added to the solution. After incubation with the probe at 37 °C for 5 min, the resulting solution was shaken well for absorption and fluorescence spectral analysis.

**D. Generation of Reactive Oxygen Species.**

Various oxidants were generated in the following procedure.

(a) Alkyl peroxyl radical ($ROO\cdot$) was generated by 2,2'-Azobis(2-amidinopropane) dihydrochloride. 2,2'-Azobis(2-amidinopropane) dihydrochloride (300 μM) was added and the mixtures were stirred at 25 °C for 1 hour;

(b) $^1O_2$ was generated by 3-(1,4-dihydro-1,4-epidioxy-1-naphthyl) propionic acid). (3-(1,4-dihydro-1,4-epidioxy-1-naphthyl) propionic acid) (final 300 μM) was added and the mixtures were stirred at 25 °C for 1 hour;

(c) $H_2O_2$ (final 300 μM) was added and the mixtures were stirred for 1 hour at 25 °C;

(d) Nitric oxide ($NO\cdot$) was generated by SNP (Sodium Nitroferricyanide (III) Dihydrate) (final 300 μM) and the mixtures were stirred for 1 hour at 25 °C;

(e) Hypochlorite anion ($ClO^-$) was generated that NaClO (final 300 μM) was added at 25 °C;

(f) Hydroxyl radical ($\cdot OH$) was generated through Fenton reaction by different amounts of $Fe^{2+}$ and $H_2O_2$ ($Fe^{2+}/H_2O_2$ = 1:6);

(g) Peroxynitrite ($ONOO^-$) (final 300 μM) was determined by UV at 302 nm, and then added at 25 °C.

**E. Time-resolved fluorescence spectroscopy.**

Fluorescence lifetimes were detected by a FLS920. Fluorescence decay traces of COF-TpMA (MC) (grinding 12 h) at various concentrations of •OH (0, 10, 100 μM) in DMSO/PBS (1:9 v/v, 40 mM, 3 mM CTAB, pH 7.4) at 37 ˚C were tracked by single-photon timing (SPT) (Figure S17). The decay times $\tau_i$ and $\alpha_i$ of COF-TpMA (MC) solution were confirmed by single decay surface recorded at 5 min after •OH addition at different $\lambda_{em}$ but at the same $\lambda_{ex}$ (400 nm). Fluorescence decay histograms were recorded using the time-correlated single photon counting technique in 4096 channels through a FLS920 spectrometer equipped with a supercontinue white laser (400-700 nm). Histograms of the instrument response functions (using LUDOX scatterer) and sample decays were obtained until it typically reached $1.0\times10^4$ counts [2]. Using FAST software to fit decay traces investigated at different $\lambda_{em}$ to get $\tau_i$ and $\alpha_i$, a global analysis of the three decay traces could provide a higher accuracy $\tau_i$ and $\alpha_i$ than a single curve analysis.

**F. Cytotoxicity tests.**

The cytotoxic activity experiment of complex against BHK cells was tested according to standard 3-(4,5-diethylthiazol-2-yl)-5-(3-carboxymethoxyphenyl)-2-(4-sulfophenyl)-2H-etrazolium, inner salt (MTS) assay procedures. BHK cells were seeded in 96-well assay plates at a density of $10^4$ cells per well (100 μL total volume/well) for 24 h. The as-prepared COF-TpMA (MC), (0, 30, 60, 90, 160 and 200 μg/mL) were added in the serum-free medium and incubated with the cells for 24 h after that. The control experiment was finished by detecting the growth culture medium without COF-TpMA (MC). The optical absorbance of the cells was detected at 490 nm through a microplate reader (German Berthold Mithras2LB943).

**G. Cell culture, fluorescence imaging.**

To obtain the cell permeability of COF-TpMA (MC), BHK cells were cultured in DMEM (Dulbecco's Modified Eagle Medium) subjoined with 10% FBS (fetal bovine serum). The cell lines were kept in a moist atmosphere containing 5% $CO_2$ at 37 °C. Cells were incubated with COF-TpMA (MC) (60 μg/mL) in 1.0 mL of fresh culture medium for 3 h with 0.5 mM CTAB after removal of the culture medium. Two sets of control experiments of BHK cells which treated with and without •OH were executed. Cells were incubated and rinsed with phosphate-buffered saline (PBS) three times to remove free compound before imaging. Confocal fluorescence images of BHK cells were carried out on an Olympus FV1000-IX81 laser confocal microscope.

## 4. Supporting Figures

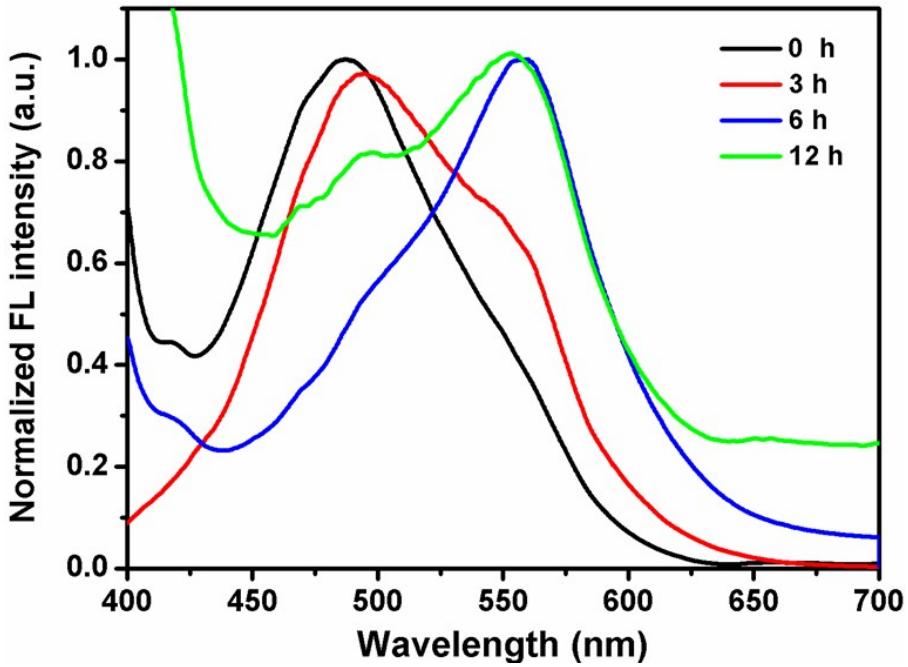


**Figure S1.** Fluorescence spectra detected at 0 h, 3 h, 6 h and 12 h during COF-TpMA (MC) synthesis.

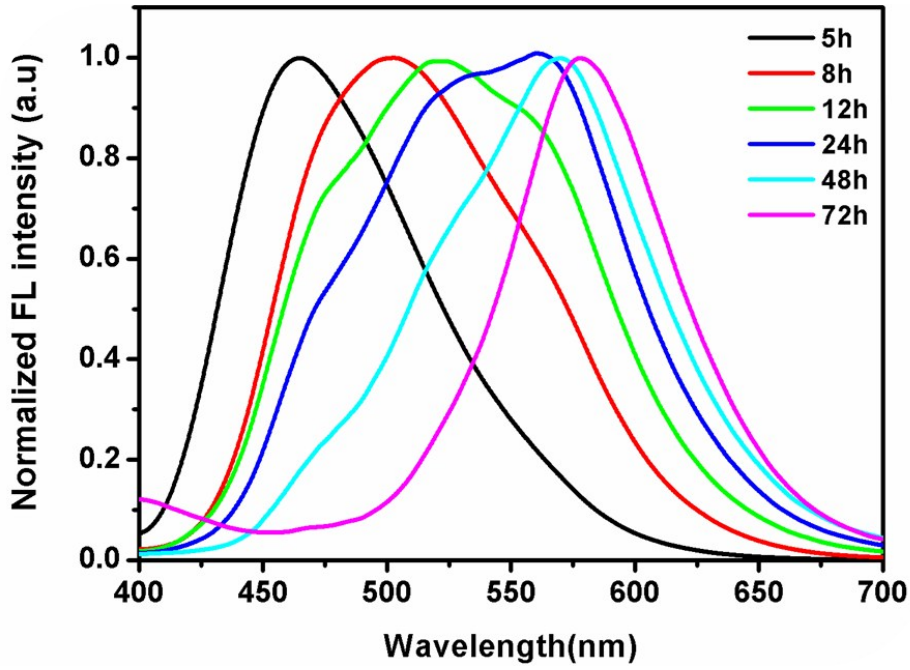


**Figure S2.** Fluorescence spectra of hydrothermal synthesis of COF TPMA in the reaction solution (mesitylene/1,4-dioxane/3 M acetic acid (5/5/1 by vol.) were detected at different times.

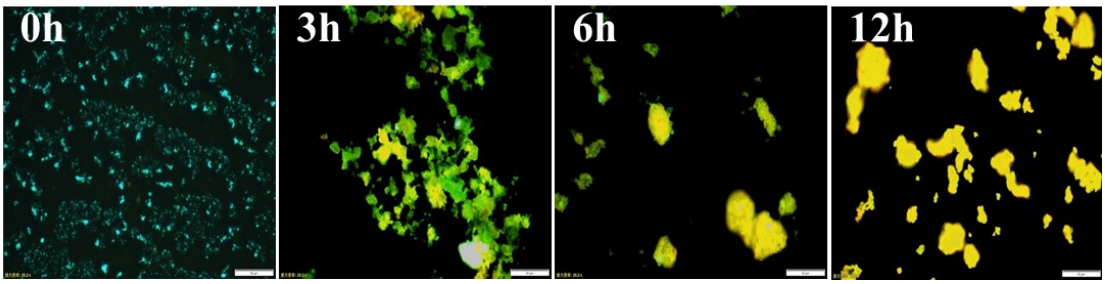


**Figure S3.** Fluorescence micrographs detected at 0 h, 3 h, 6 h and 12 h during COF-TpMA (MC) synthesis.

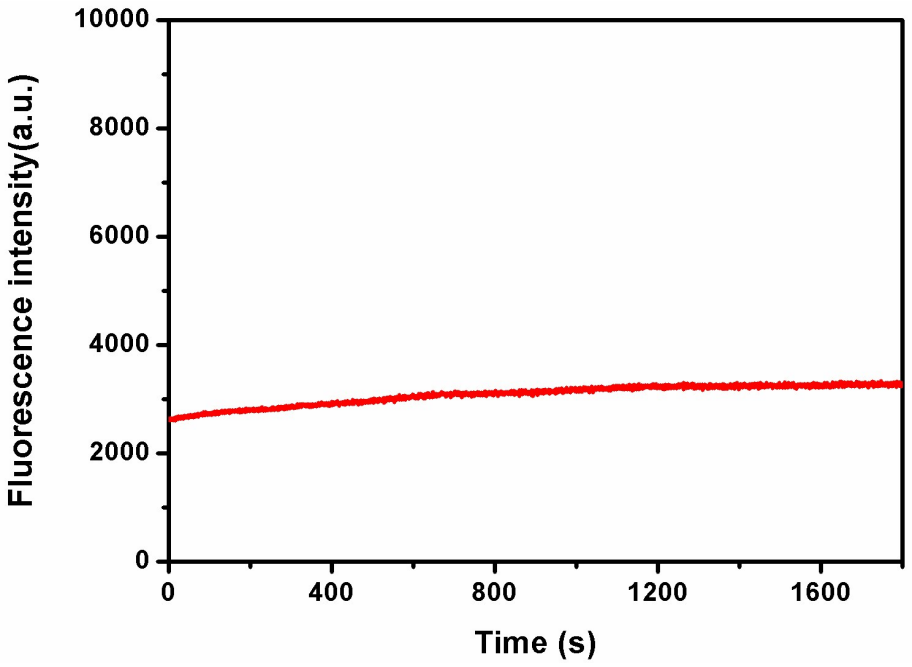


**Figure S4.** Photo-stability of COF-TpMA (MC) in solution.

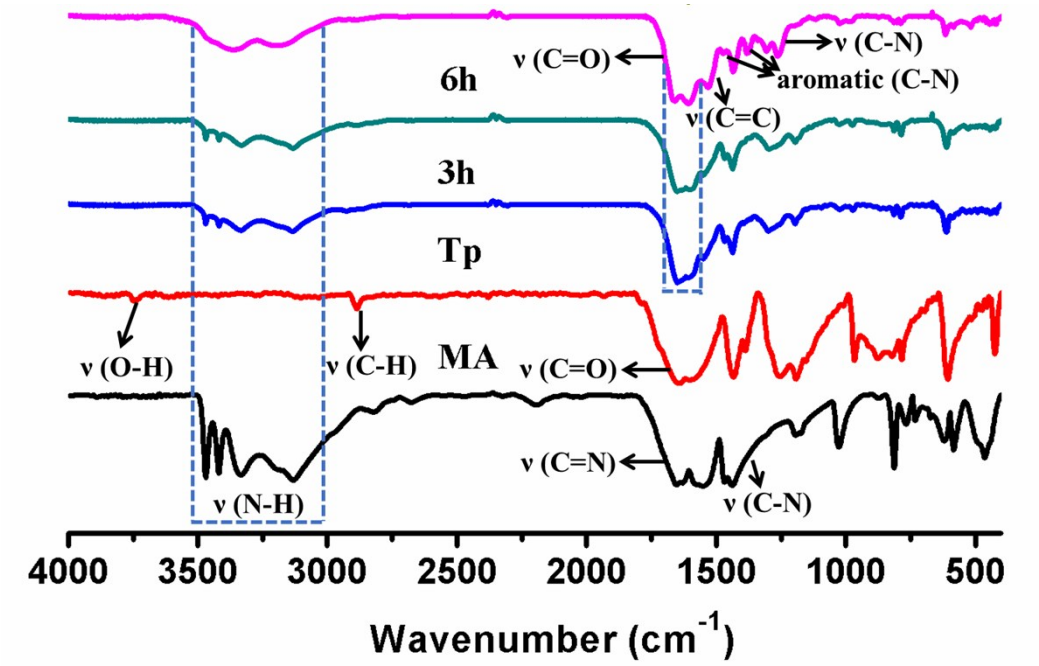


**Figure S5.** IR spectra detected at 0 h, 3 h, 6 h and 12 h during COF-TpMA (MC) synthesis.

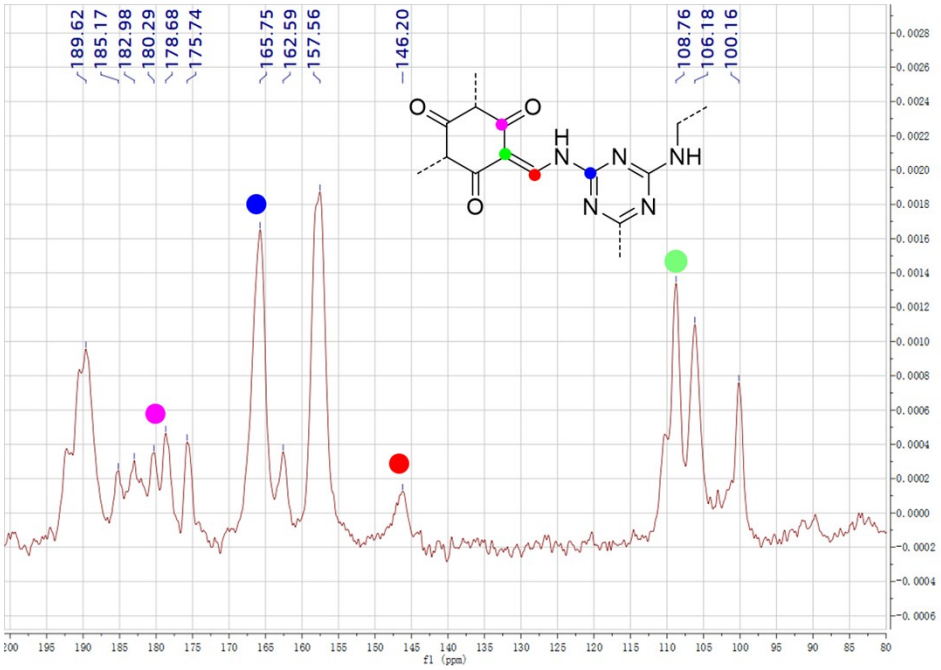


**Figure S6.**[13] C CP-MAS NMR spectrum of COF-TpMA (MC).

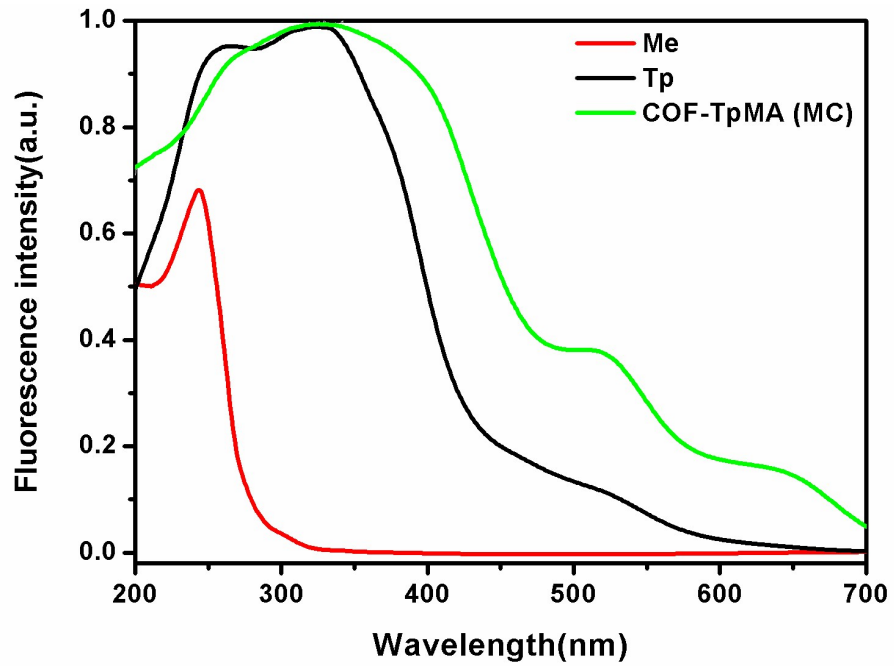


**Figure S7.** UV/vis absorption spectra (in the solid state) of COF-TpMA (MC) (red line) and Tp (pink line).

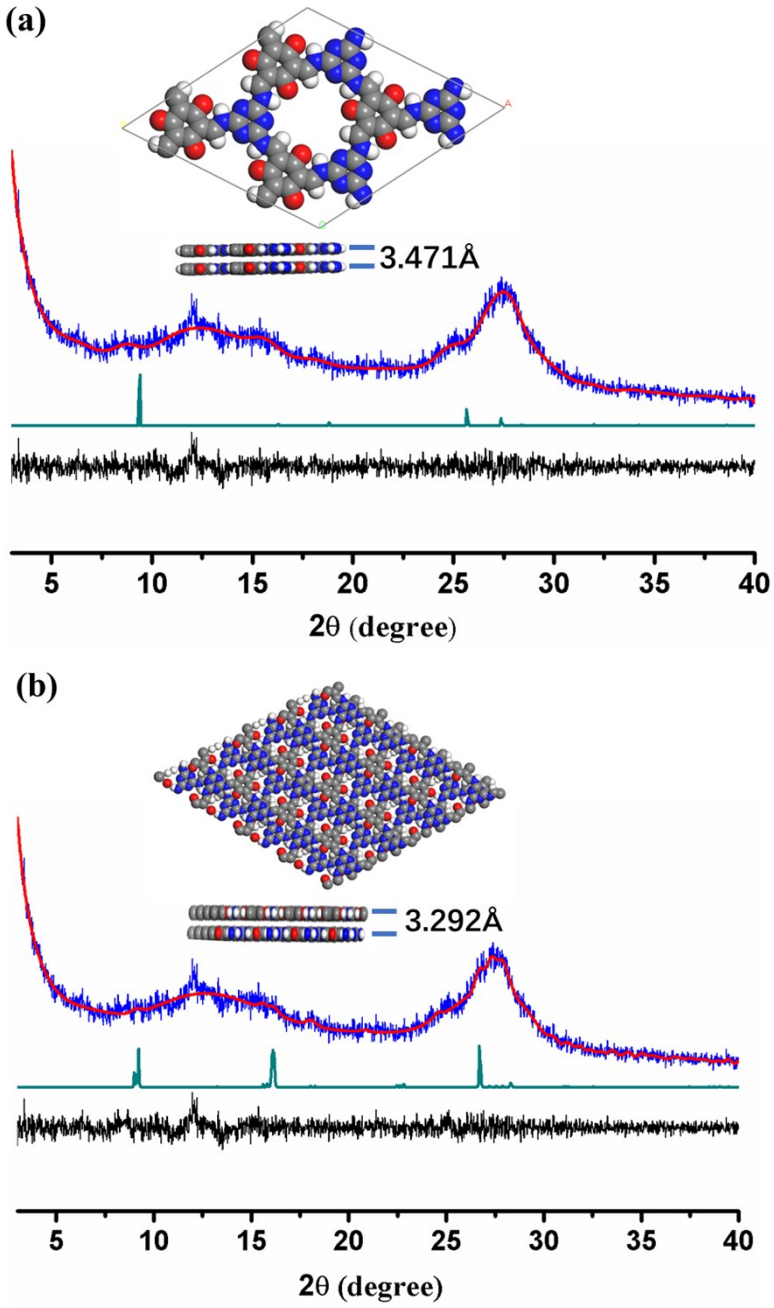


**Figure S8.** Top views of the AA stacking (a) and AB stacking (b) structure of COF-TpMA (MC), bottom views of the XRD pattern of COF-TpMA: experimental result (blue), simulated of AA-stacking (green), Pawley refinement (red), and associated difference (black).

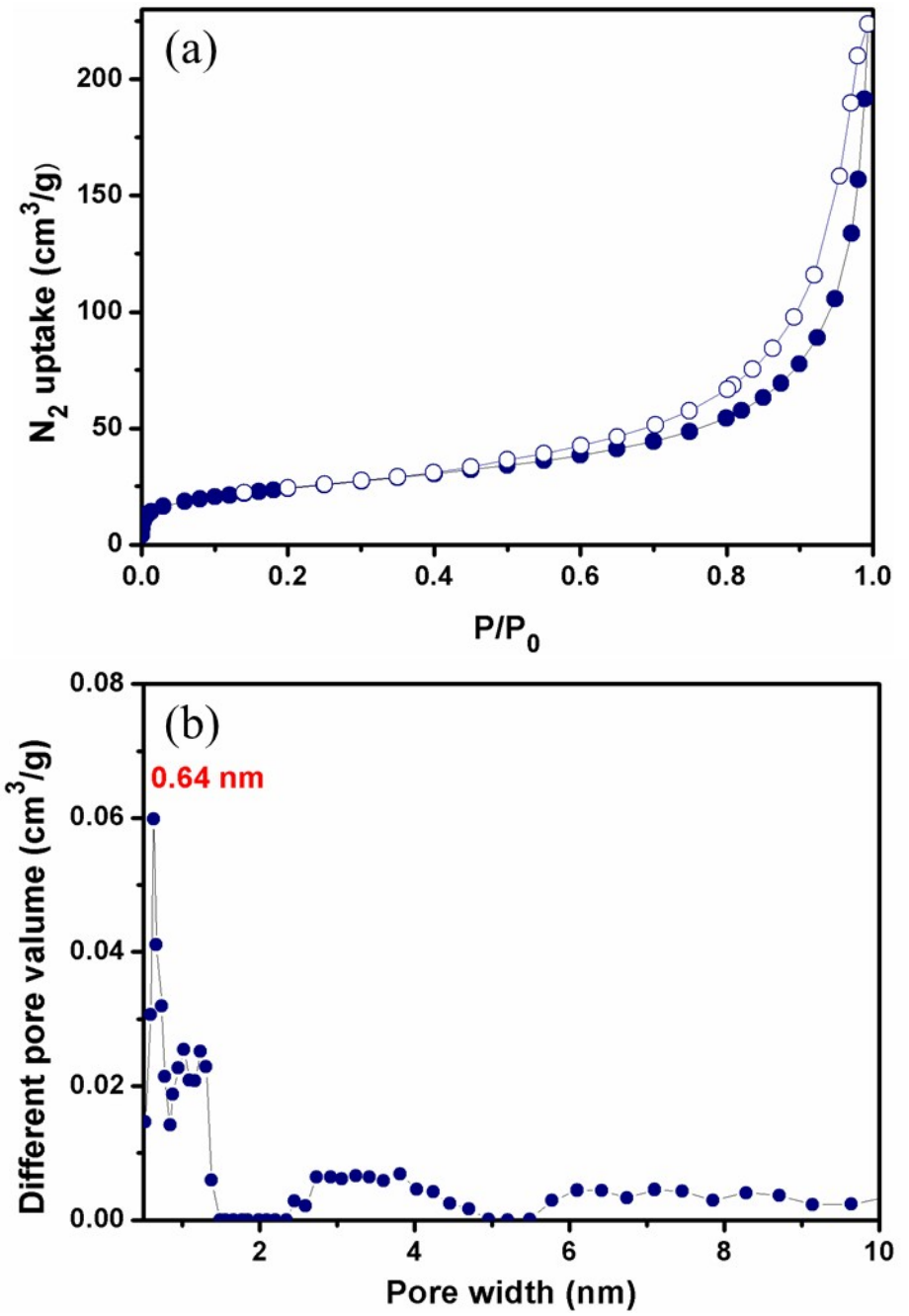


**Figure S9.** (a) $N_2$ adsorption-desorption isotherms and (b) pore size distribution profiles of COF-TpMA (MC).

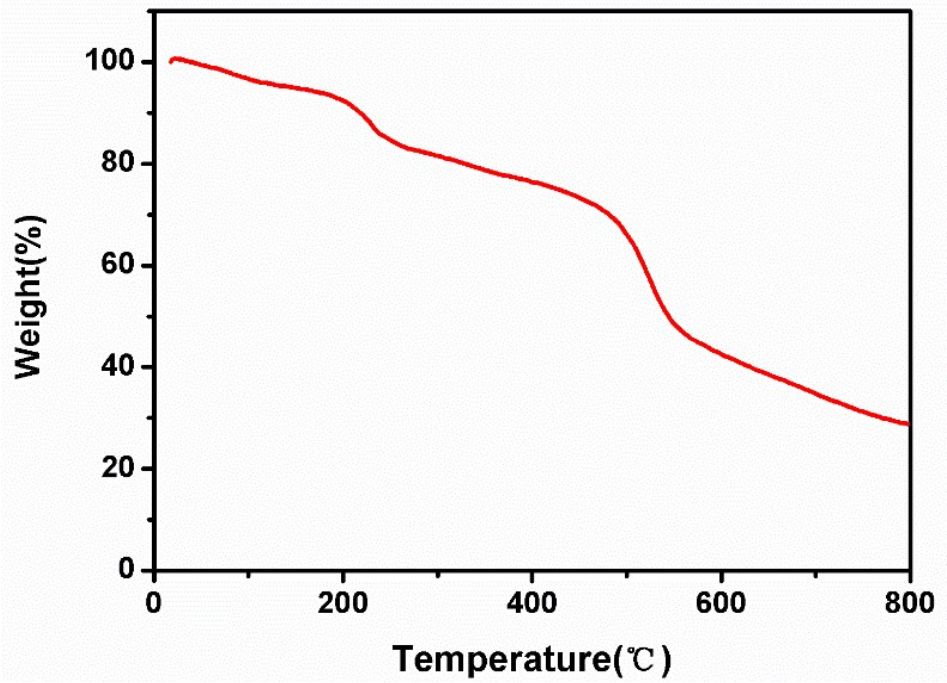


**Figure S10.** TGA curve of COF-TpMA (MC).

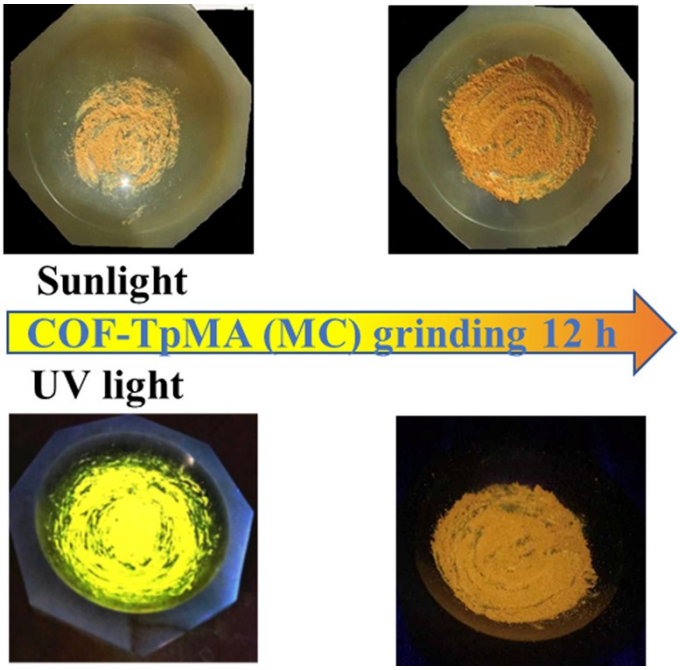


**Figure S11.** Photo of products under sunlight (Top) and UV light (Bottom) of COF-TpMA (MC) at 12 grinding.

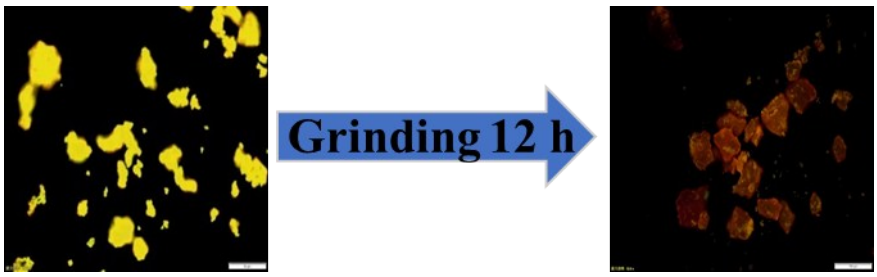


**Figure S12.** Fluorescence micrographs of COF-TpMA (MC) and COF-TpMA (MC) after grinding for 12 h.

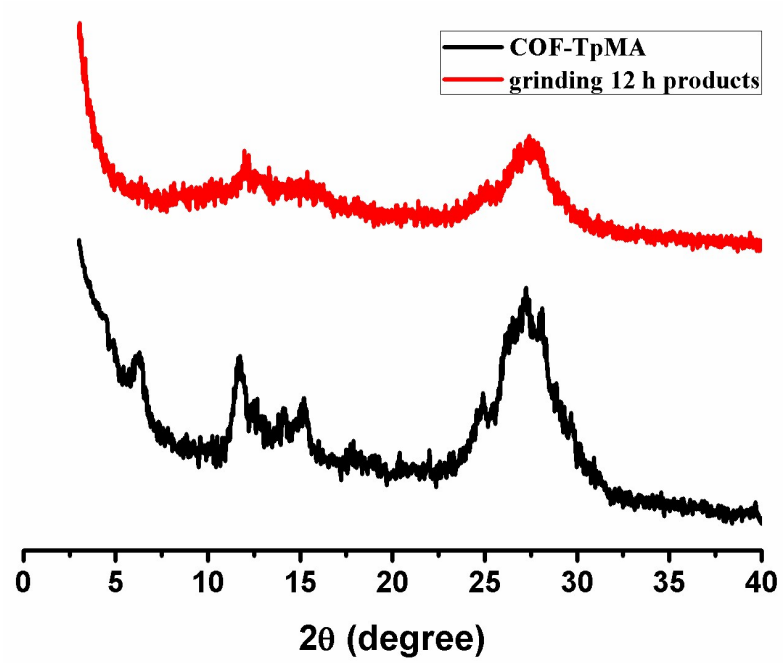


**Figure S13.** The PXRD spectra of COF-TpMA (MC) and grinding 12 h product.

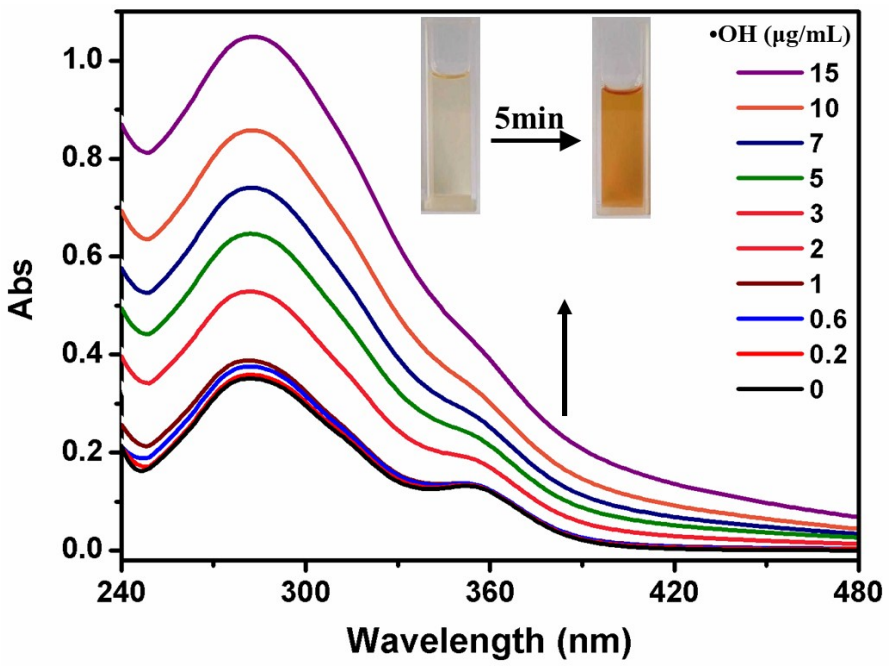


**Figure S14.** Absorption spectra of COF-TpMA (MC) in different concentration of •OH.

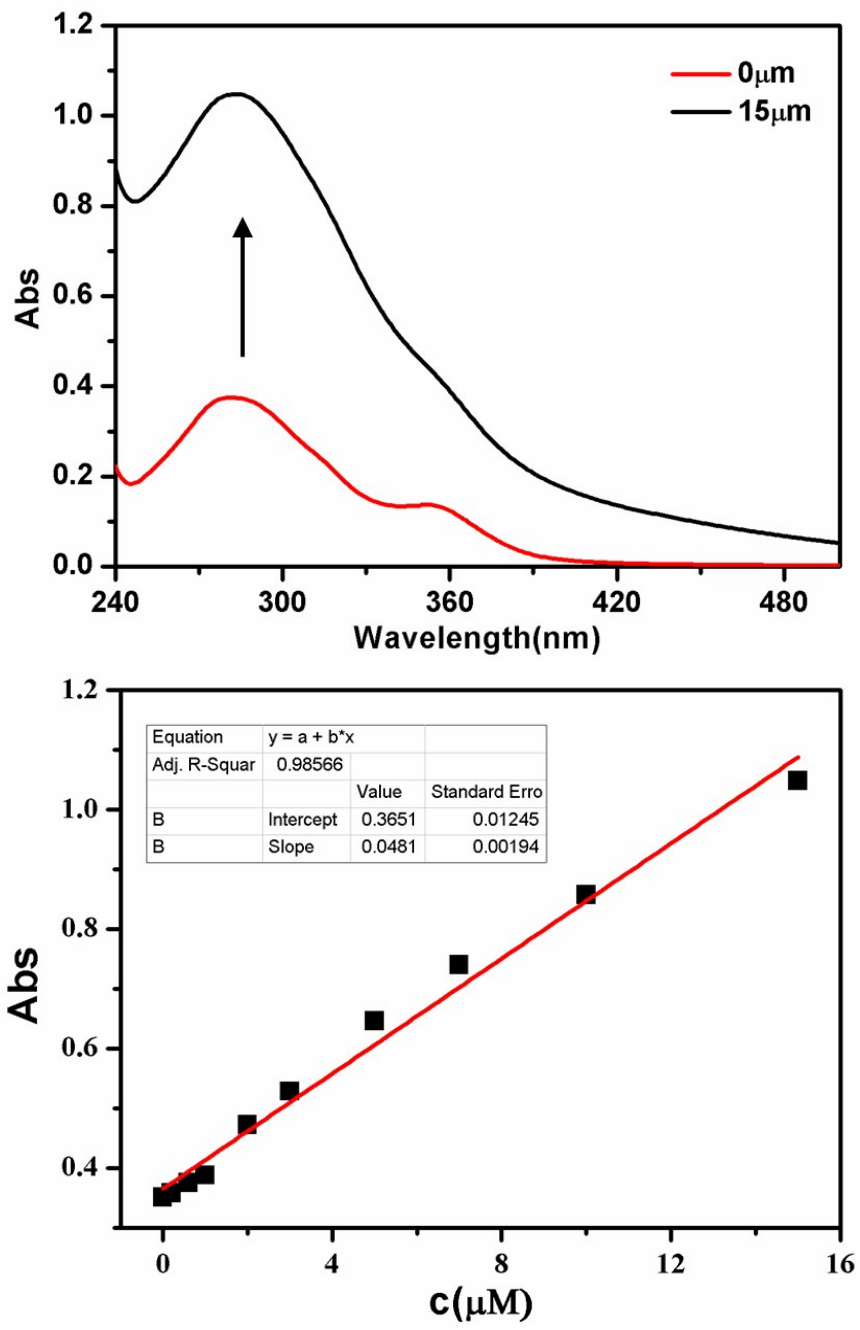


**Figure S15.** (a) Absorption changes of COF-TpMA (MC) (60 μg/mL) with •OH and (b) the linear relationship between the •OH concentration range (0-10μM) at 283nm.

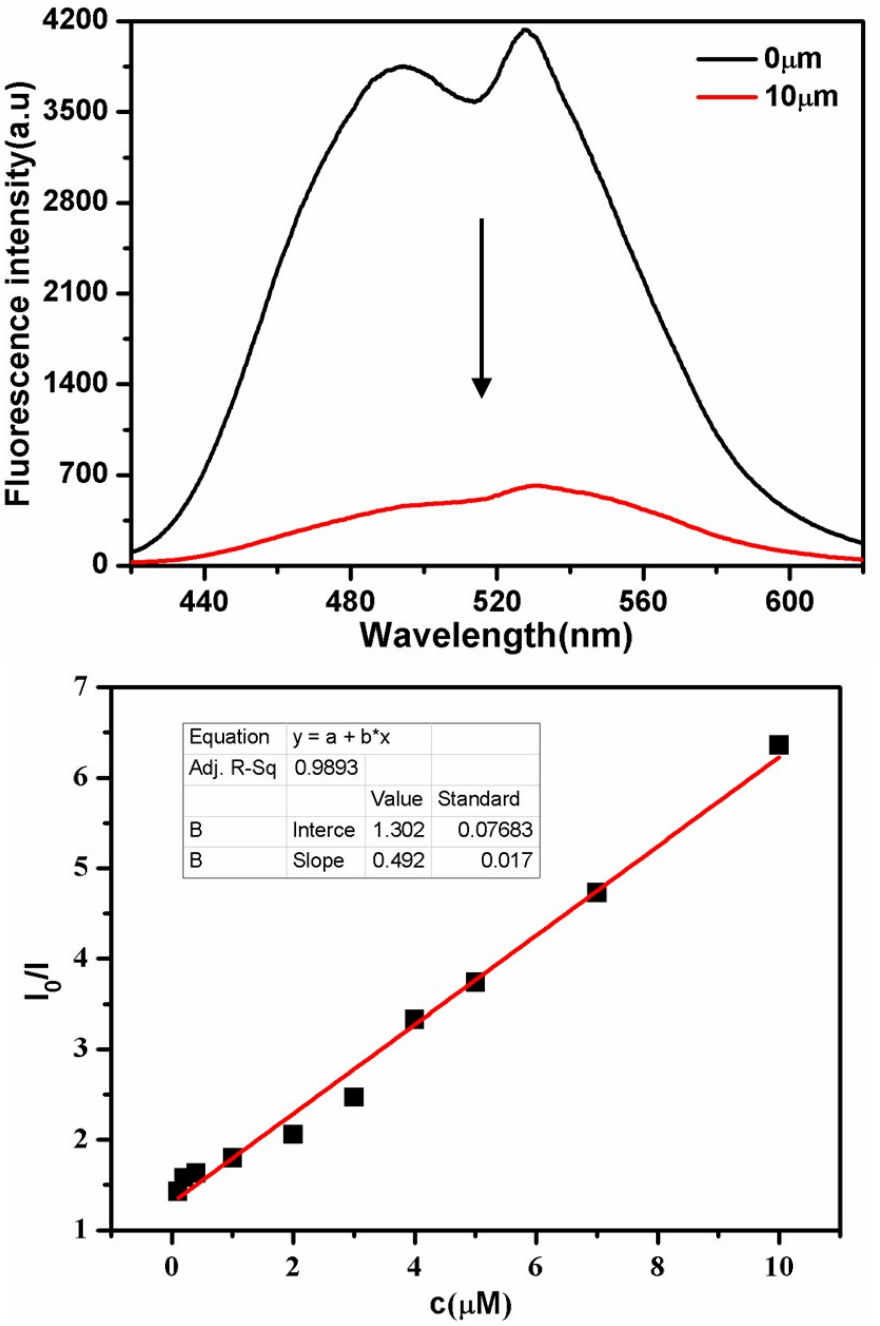


**Figure S16.** (a) Fluorescence changes of COF-TpMA (MC) (60 μg/mL) with •OH and (b) the linear relationship between the •OH concentration range (0-10μM) at 530nm (λex = 380nm).

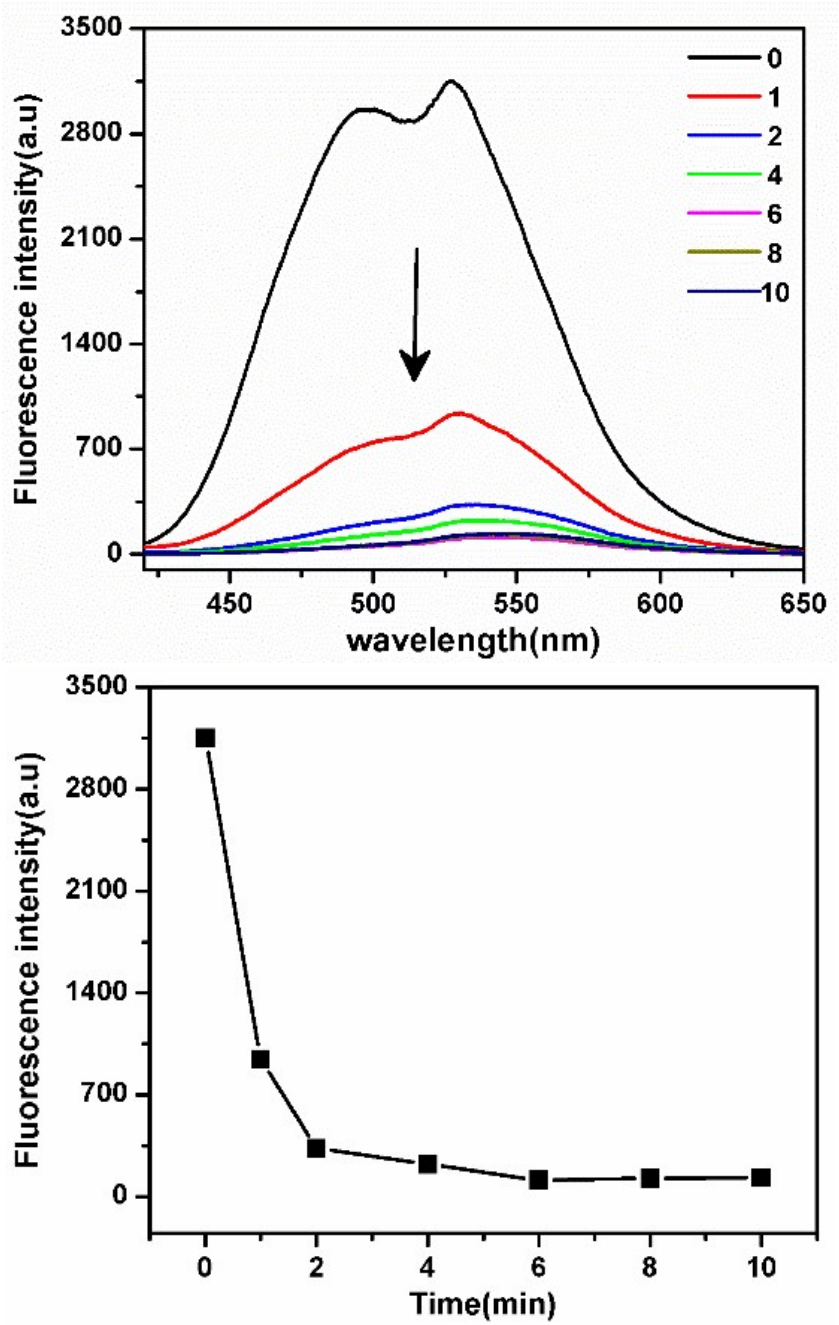


**Figure S17.** Time-dependent fluorescent response at 530 nm (λex = 380nm) for COF-TpMA (MC) (60 μg/mL) upon addition of 10 μM of •OH.

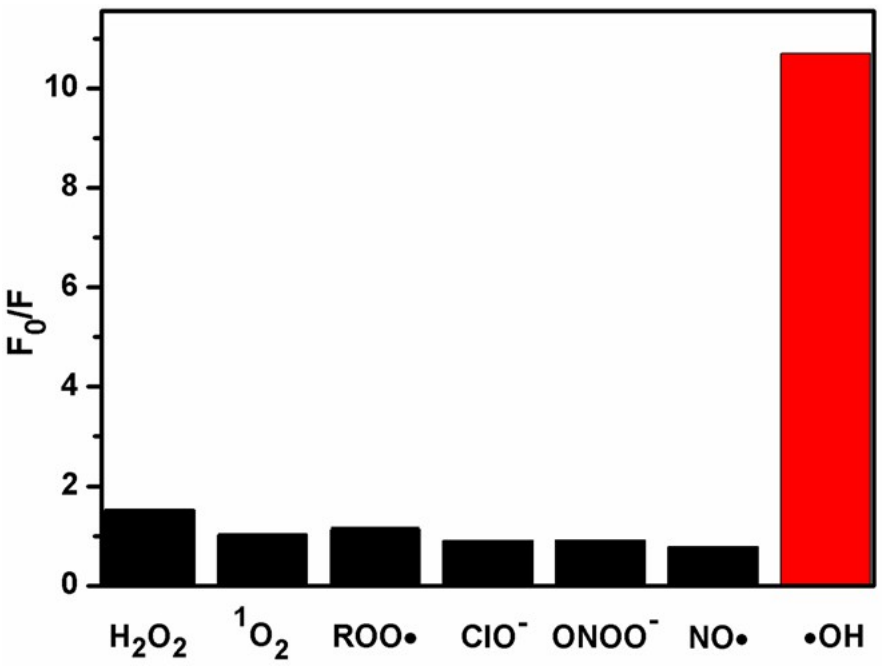


**Figure S18.** Specific selectivity of COF-TpMA (MC) (0.022 mg/mL) reacted with different reactive oxygen species (150 μM).

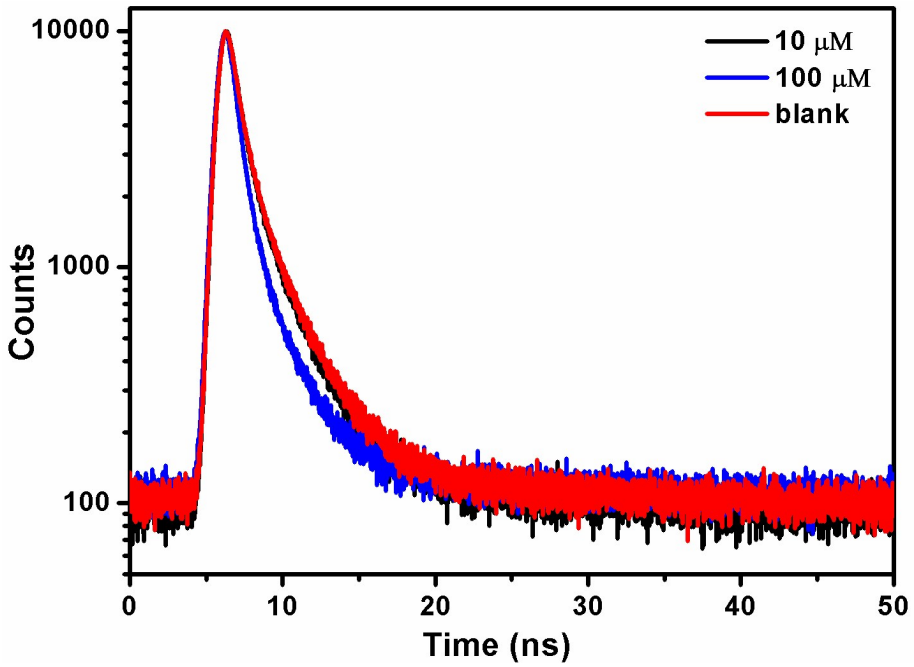


**Figure S19.** Representative fluorescence decays of COF-TpMA (MC) (60 μg/mL) in the absence and presence of different concentration of •OH. All traces were obtained after 5 min of incubation with •OH in PBS buffer (20 mM, pH 7.4) with 3 mM CTAB.

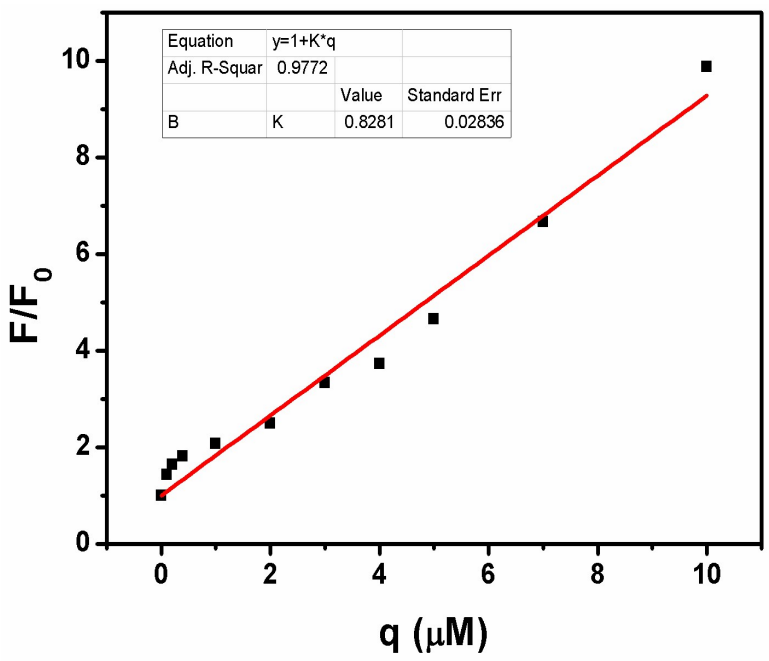


**Figure S20.** Best fits of Eq $F/F_0=1+Kq$ to the emission fluorometric titration data (530 nm) of COF-TpMA in PBS buffered solution with •OH ranging from 0-10 μM ($F_0$ and F are the fluorescence intensity of •OH at concentration q μM and 0 μM).

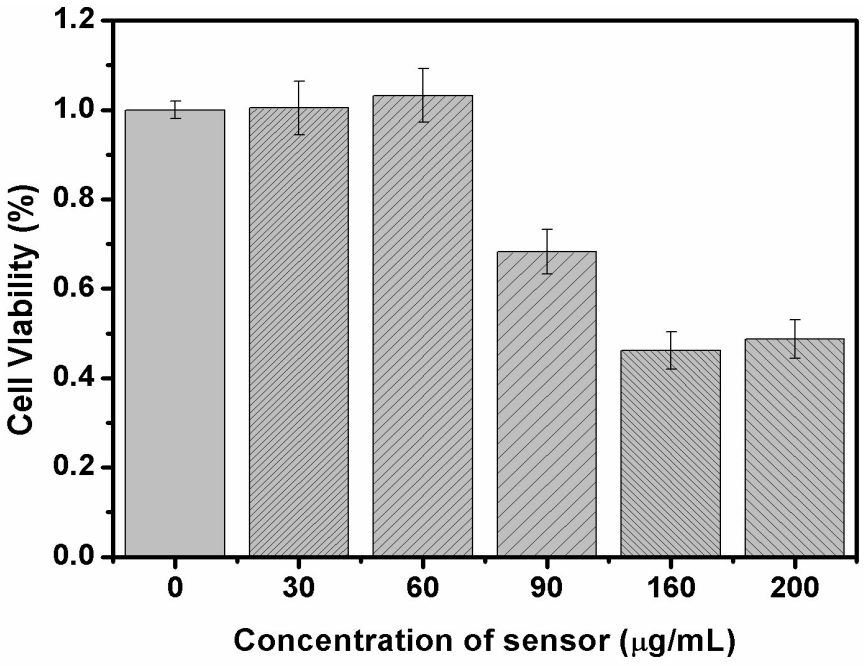


**Figure S21.** Effects of COF-TpMA at varied concentrations on the viability of BHK cells. The cell viability data were checked three times.

## 5. Supporting Tables

**Table S1.** Fractional atomic coordinates for the unit cell of COF-TpMA of AA stacking.

| **COF-TpMe AA stacking model** | | | | | | | |
|---|---|---|---|---|---|---|---|
| **Hexagonal P-6** | | | | | | | |
| **a=b=10.8876Å, c=3.4708Å; α=β=90°, γ=120°** | | | | | | | |
| C1 | 0.18175 | 0.62303 | 0.5 | C6 | 0.79964 | 0.39550 | 0.5 |
| C2 | 0.23274 | 0.52487 | 0.5 | O7 | 0.59686 | 0.74518 | 0.5 |
| C3 | 0.41202 | 0.45859 | 0.5 | H8 | 0.33634 | 0.34884 | 0.5 |
| N4 | 0.54422 | 0.48488 | 0.5 | H9 | 0.62485 | 0.58110 | 0.5 |
| N5 | 0.74097 | 0.47258 | 0.5 | | | | |

**Table S2.** Fractional atomic coordinates for the unit cell of COF-TpMA of AB stacking.

| **COF-TpMe AB stacking model** | | | | | | | |
|---|---|---|---|---|---|---|---|
| **Triclinic P1** | | | | | | | |
| **a=6.6720Å, b=11.3484Å, c=11.0797Å; α=120°, β=γ=90°** | | | | | | | |
| C1 | 0.62598 | 0.20561 | 0.775 | C28 | 0.98261 | 0.83501 | 0.29197 |
| C2 | 0.77495 | 0.27233 | 0.775 | C29 | 0.13159 | 0.90173 | 0.29197 |
| C3 | 0.99876 | 0.47480 | 0.775 | C30 | 0.35540 | 0.10419 | 0.29197 |
| N4 | 0.10176 | 0.61650 | 0.775 | N31 | 0.45840 | 0.24590 | 0.29197 |
| N5 | 0.33459 | 0.79256 | 0.775 | N32 | 0.69122 | 0.42196 | 0.29197 |
| C6 | 0.46706 | 0.83418 | 0.775 | C33 | 0.82369 | 0.46358 | 0.29197 |
| O7 | 0.86823 | 0.63155 | 0.775 | O34 | 0.22486 | 0.26095 | 0.29197 |
| H8 | 0.03407 | 0.40346 | 0.775 | H35 | 0.39070 | 0.03286 | 0.29197 |
| H9 | 0.08233 | 0.69567 | 0.775 | H36 | 0.43897 | 0.32507 | 0.29197 |
| C10 | 0.86356 | 0.42340 | 0.775 | C37 | 0.22020 | 0.05279 | 0.29197 |
| C11 | 0.79915 | 0.50815 | 0.775 | C38 | 0.15578 | 0.13755 | 0.29197 |
| C12 | 0.60122 | 0.53214 | 0.775 | C39 | 0.95786 | 0.16154 | 0.29197 |
| N13 | 0.45250 | 0.50495 | 0.775 | N40 | 0.80914 | 0.13435 | 0.29197 |
| N14 | 0.28081 | 0.56485 | 0.775 | N41 | 0.63744 | 0.19425 | 0.29197 |
| C15 | 0.24105 | 0.65811 | 0.775 | C42 | 0.59769 | 0.28751 | 0.29197 |
| O16 | 0.44470 | 0.24034 | 0.775 | O43 | 0.80134 | 0.86973 | 0.29197 |
| H17 | 0.67219 | 0.64031 | 0.775 | H44 | 0.02883 | 0.26971 | 0.29197 |
| H18 | 0.37396 | 0.40508 | 0.775 | H45 | 0.73059 | 0.03448 | 0.29197 |
| C19 | 0.65062 | 0.44598 | 0.775 | C46 | 0.00726 | 0.07537 | 0.29197 |
| C20 | 0.56606 | 0.29450 | 0.775 | C47 | 0.92270 | 0.92390 | 0.29197 |
| C21 | 0.54018 | 0.06804 | 0.775 | C48 | 0.89681 | 0.69744 | 0.29197 |
| N22 | 0.56668 | 0.97603 | 0.775 | N49 | 0.92331 | 0.60543 | 0.29197 |
| N23 | 0.50555 | 0.74008 | 0.775 | N50 | 0.86219 | 0.36948 | 0.29197 |
| C24 | 0.41283 | 0.60519 | 0.775 | C51 | 0.76947 | 0.23459 | 0.29197 |
| O25 | 0.82724 | 0.20310 | 0.775 | O52 | 0.18388 | 0.83249 | 0.29197 |
| H26 | 0.43391 | 0.03120 | 0.775 | H53 | 0.79054 | 0.66060 | 0.29197 |
| H27 | 0.66465 | 0.99674 | 0.775 | H54 | 0.02129 | 0.62613 | 0.29197 |

**Table S3.** Photophysical Properties of 1 in the absence and in addition of •OH in DMSO/PBS buffer (1:9, v/v, 0.022 mg/mL, 3 mM CTAB, pH 7.4) at 37 ˚C. Global analyses of decay times $\tau_1$, $\tau_2$ and $\tau_3$, and the relative amplitude $\alpha$i (%), each spectrum was recorded 5 min after •OH addition at the same excitation wavelength (380 nm), but at different emision wavelength.

| Addition of •OH/μM | Measured wavelength/nm | $\tau_1$/ns | $\tau_2$/ns | $\tau_3$/ns | $\alpha_1$ (%) | $\alpha_2$ (%) | $\alpha_3$ (%) |
|---|---|---|---|---|---|---|---|
| 0 | 515 | 0.435±0.0304 | 1.410±0.0112 | 3.580±0.0032 | 33.21 | 46.25 | 20.54 |
| | 525 | | | | 31.27 | 44.72 | 24.01 |
| | 535 | | | | 30.48 | 44.29 | 25.24 |
| 10 | 515 | 0.410±0.0320 | 1.333±0.0113 | 3.432±0.0031 | 33.09 | 45.99 | 20.93 |
| | 525 | | | | 30.75 | 45.34 | 23.90 |
| | 535 | | | | 30.78 | 43.70 | 25.52 |
| 100 | 515 | 0.371±0.0311 | 1.3915±0.0118 | 3.732±0.0043 | 44.92 | 44.35 | 10.73 |
| | 525 | | | | 41.83 | 45.46 | 12.71 |
| | 535 | | | | 43.10 | 43.58 | 13.32 |

## 6. Supporting References

1. Ding, S.-Y.; Gao, J.; Wang, Q.; Zhang, Y.; Song, W.-G.; Su, C.-Y.; Wang, W., Construction of Covalent Organic Framework for Catalysis: Pd/COF-LZU1 in Suzuki–Miyaura Coupling Reaction. *Journal of the American Chemical Society* **2011,** 133, (49), 19816-19822.

2. Biswal, B. P.; Chandra, S.; Kandambeth, S.; Lukose, B.; Heine, T.; Banerjee, R., Mechanochemical synthesis of chemically stable isoreticular covalent organic frameworks. *J Am Chem Soc* **2013,** 135, (14), 5328-5331.

3. Olmsted, J. J. Phys. Chem. 1979, 83, 2581-2584.